

Finite-Size Analysis of the Collapse of Dry Granular Columns

Teng Man

*Institute of Advanced Technology, Westlake Institute for Advanced Study,
18 Shilongshan Street, Hangzhou, Zhejiang 310024, China**

Herbert E. Huppert

*Institute of Theoretical Geophysics, King's College, University of Cambridge,
King's Parade, Cambridge CB2 1ST, United Kingdom*

Ling Li and Sergio Andres Galindo-Torres[†]

*Key Laboratory of Coastal Environment and Resources of Zhejiang Province (KLaCER),
School of Engineering, Westlake University, 18 Shilongshan Street, Hangzhou, Zhejiang 310024, China*

(Dated: July 22, 2022)

The collapse of granular columns is potentially connected to the dynamics of complex flows, such as debris flows, landslides, and particulate flows in chemical engineering and food processing, yet the link between the microscopic structures of granular assemblies and their macroscopic behaviors is still not fully understood. In this paper, we focus on the size effect of granular column collapses using the sphero-polyhedral discrete element method (DEM) to show that the ratio between column radius and the grain size has a strong influence on the collapse behavior. The finite-size scaling analysis, which is inspired by a phase transition of granular column collapses around an inflection point, is performed to obtain a general scaling equation with critical exponents for the run-out distance of the granular column collapses. We further link the size effect with the strong force network and formalize a correlation length scale which exponentially scales with the effective aspect ratio. Such a scaling solution shows similarities with that of the percolation problem of two-dimensional random networks and can be extended to other similar natural and engineering systems.

Usage: Secondary publications and information retrieval purposes.

Structure: You may use the `description` environment to structure your abstract; use the optional argument of the `\item` command to give the category of each item.

Introduction.— Granular materials are omnipresent in both natural and engineering systems, and the physics and mechanics of them are crucial for understanding some aspects of geophysical flows, natural hazards (such as debris flows, landslides, and pyroclastic flows), food processing, chemical engineering, and pharmaceutical engineering[1]. Granular materials can behave like a solid, a liquid, or a gas in different circumstances[2], which increases the difficulty in capturing the macroscopic behavior of them. Besides, collective structures may form inside a granular system, and the existence and the size of such collective structures (such as bridging[3], granular agglomerates[4], and contact networks[5]) will introduce a strong size effect into the macroscopic behavior of granular materials, which further increases the complexity of the problem. In recent decades, breakthroughs have been made to understand the basic governing principles, especially the constitutive relationships, of granular materials[2, 6–10], where the behavior of granular materials or granular-fluid mixtures were considered to be described by dimensionless numbers expressed as the ratio between dominating stresses.

Due to the similarity and potential links between the collapse of granular columns and gravity-driven geophysical flows, such as debris flows, landslides, and rock avalanches, previous research investigated the collapse of granular columns to analyze the post-failure behav-

ior of granular systems [11–15]. Lube et al.[16, 17] and Lajeunesse et al.[18] independently determined relationships for both the normalized run-out distance $\mathcal{R} = (R_\infty - R_i)/R_i$ (where R_∞ is the final radius of the granular pile, and R_i the initial radius of the granular column), and the halt time of a collapsed granular column scale with the initial aspect ratio, $\alpha = H_i/R_i$ (where H_i is the initial height) of the column, a parameter drawn out of the dimensional analysis. Warnett et al.[19, 20] and Cabrera et al.[21] studied the collapse of granular columns with experiments and simulations, respectively, and argued that the relative size of a granular column, R_i/d , has a strong influence on the run-out distance of a collapsed granular column, and to avoid significant size effects, R_i/d must be larger than 75 for short columns and larger than 50 for tall columns.

Based on these studies, the authors [22] investigated the collapse of axisymmetric granular columns and their resulting deposition morphology with a wide range of inter-granular and particle/boundary frictional coefficients, and concluded that the normalized run-out distance, \mathcal{R} , scales with an effective aspect ratio, $\alpha_{\text{eff}} = \sqrt{1/(\mu_w + \beta\mu_p)}(H_i/R_i)$, where μ_w is the frictional coefficient between particles and the boundary, μ_p is the inter-particle frictional coefficient, and β is a fitting parameter, where the best value was determined to be 2.0. They found that the collapse of granular columns can be

classified into three different regimes: quasi-static, inertial, and liquid-like. The effective aspect ratio, which was used to describe the run-out behavior, was obtained from dimensional analysis and was shown to represent the ratio between the inertial stress and the frictional stress or, equivalently, the ratio between the kinetic energy and dissipated energy during the collapse of granular columns [22].

In this paper, we further conducted a systematic study of granular column collapses with the sphero-polyhedral discrete element method (DEM) to study the influence of relative column size on the run-out distance to obtain a scaling solution to describe granular column collapses with different sizes.

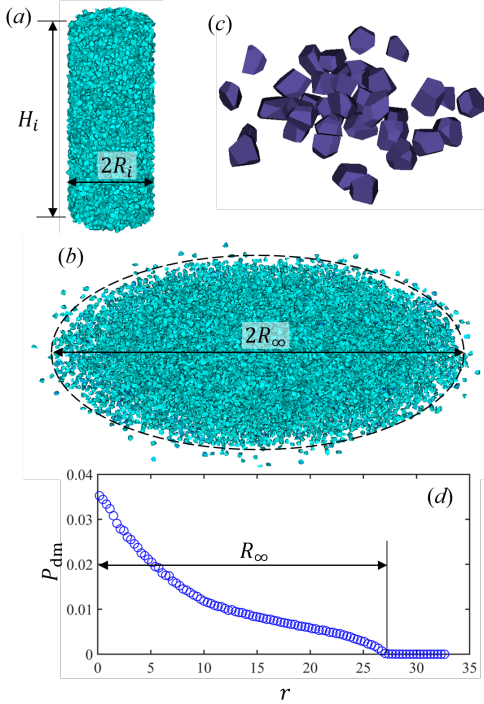


FIG. 1. Simulation set-up. (a) shows the initial state of the granular column; (b) shows the final deposition of the collapsed column in a 3-D view; and (c) represents Voronoi-based particles in the DEM simulation; (d) shows the method for measuring the run-out distance of a collapsed granular column. The x -axis is the radial position r , and the y -axis is the percentage of number of particles, P_{dm} , located within $(r - \Delta r/2, r + \Delta r/2)$ divided by the radial position. We measure the final radius of a collapsed granular column when $P_{dm}(r) \leq 5\% P_{dm}^{\max}$.

Simulation set-up.— We perform DEM simulations of the granular column collapses with sphero-polyhedra particles. The model has been thoroughly validated with experiments in our previous research [22, 23]. In the simulation, we create particles in a certain cylindrical domain [24], with initial height, H_i , and initial radius, R_i [FIG. 1(a)]. 20% of the particles are randomly chosen and removed from the simulation to create a granular pack-

ing with an initial solid fraction of $\phi_s = 0.8$. The average particle size d is 0.2 cm. The coefficient of restitution of particle collisions is 0.1. The material properties are set to be the same as that of quartz sand (particle density 2.65 g/cm^3). This paper entirely focuses on simulations with granular columns of circular cross-sections. More general cross-sections are currently under investigation and will be presented in a subsequent publication. The particle/boundary frictional coefficient μ_w is 0.4, while the inter-particle frictional coefficients μ_p are 0.2, 0.4, and 0.6.

We treat the relative column size ($R_i/d = 2, 2.5, 3.75, 5, 7.5, 10, 12.5, 15, 17.5, 20, 30$) as a key parameter. Within one set of simulations, with the same R_i/d , we varied the initial height H_i and the inter-particle frictional coefficient μ_p to obtain the general collapse behavior with a wide range of initial conditions. After releasing particles to the horizontal plane, the granular material will form a pile of loosely packed grains [FIG. 1(b)], with final packing radius, R_∞ . Thus, the normalized run-out distance, $\mathcal{R} = (R_\infty - R_i)/R_i$, could be obtained. With Voronoi-based spheropolyhedra particles (FIG. 1(c)), we implement the Hookean contact model with an energy dissipation term to calculate the interactions among contacting particles [24]. In this paper, the contact law parameters are the same as the previous paper [22, 25]. The motion of particles is then calculated by step-wise resolution of Newton's second law.

Determination of the run-out distance.— In simulations, the measurement of the final packing radius is more complicated than that in experiments. In cases with small particle/boundary and interparticle frictional coefficients but large initial aspect ratios, the spread of particles is far-reaching and leads to sparse (single layer) coverage of the area, especially at the front edge. In these cases, it is difficult to determine the edge/boundary and hence the final run-out distance. Thus, we measured the final radius with a histogram of particle distribution for each simulation. FIG. 1(d) gives an example of how we measured the run-out distance.

In FIG. 1(d), the x -axis is the radial position r , and the y -axis is the percentage of number of particles located within $(r - \Delta r/2, r + \Delta r/2)$ divided by the radial position, $P_{dm}(r) = (1/r)[N(r - \Delta r/2, r + \Delta r/2)/(\Sigma_r N)]$, where Δr is the bin width of the histogram, and $N(r - \Delta r/2, r + \Delta r/2)$ is the number of particles located between $r - \Delta r/2$ and $r + \Delta r/2$, and $\Sigma_r N$ is the total number of particles in one simulation. FIG. 1(d) shows the normalized particle number distribution (i.e. deposition morphology) of a simulation with $\mu_w = 0.4$, $\mu_p = 0.4$, $R_i = 4 \text{ cm}$, and $H_i = 32 \text{ cm}$. It shows that most particles locate within $r \leq 27 \text{ cm}$. Thus, we take the final deposition radius as $R_\infty = 27 \text{ cm}$, and the normalized run-out distance can be calculated as $\mathcal{R} = (R_\infty - R_i)/R_i = 5.75$.

Results and discussions.— After simulating granular column collapses with various column sizes and frictional

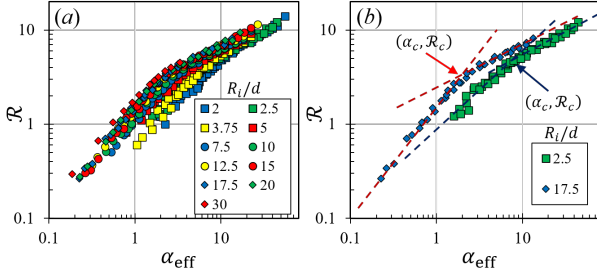


FIG. 2. (a) plots the normalized run-out distance, $\mathcal{R} = (R_\infty - R_i)/R_i$ against the effective aspect ratio, $\alpha_{\text{eff}} = \alpha\sqrt{1/(\mu_w + 2\mu_p)}$ for all the column sizes. (b) shows the relationship between \mathcal{R} and α_{eff} with relative column size $R_i/d = 2.5$ and 17.5 , respectively, to show that the critical inflection point $(\alpha_c, \mathcal{R}_c)$ changes as we change the relative size of the column.

coefficients, we obtain the relationship between \mathcal{R} and α . Similar to what we have seen in our previous research[22], for columns with the same relative size R_i/d , less friction leads to larger run-out distances. As we change the x -axis to the effective aspect ratio, α_{eff} , normalized run-out distance with the same R_i/d collapse onto one curve in $\mathcal{R} - \alpha_{\text{eff}}$ space [FIG. 2(a) and (b)]. The previous work indicates that the effective aspect ratio, which includes the influence of both initial aspect ratio and particle frictional properties, could describe the run-out behavior of the granular column collapse, and most importantly it shows that, for columns with the same relative column size, there is only one transition point for certain column size in the $\mathcal{R} - \alpha_{\text{eff}}$ relationship. The collapsing of the transition point of the $\mathcal{R} - \alpha_{\text{eff}}$ relationship indicates possible phase transition related to the collapsing dynamics of granular columns.

However, with various relative column sizes, we can see that, in both FIG. 2(a) and (b), simulation results, especially the transition point in each $\mathcal{R} - \alpha_{\text{eff}}$ relationship, varies as we change R_i/d . For granular columns with the same initial aspect ratio, granular columns with larger relative column size R_i/d have longer run-out distances. In FIG. 2(a), we plot simulation results with all the system sizes, and we plot simulation results with $R_i/d = 2.5$ and $R_i/d = 17.5$ in FIG. 2(b), and the latter can give us a clearer picture of how changing relative system size could result in variations in the relationship between \mathcal{R} and α_{eff} and variations in the transition point $(\alpha_c, \mathcal{R}_c)$. This shows that the collapse of the granular column has a significant size effect, which was also observed in the research of Warnett et al.[19] and Cabrera et al.[21]. However, no quantitative studies has been made to universally include different frictional coefficients and boundary conditions to describe the run-out behavior and few researchers pointed out the physical nature of the initial aspect ratio α other than obtaining it from dimensional analysis[22].

Further, changing the relative column size also fundamentally influences the shape of $\mathcal{R} - \alpha_{\text{eff}}$. For simulations with the same R_i/d , a threshold α_c of α_{eff} exists to divide the $\mathcal{R} - \alpha_{\text{eff}}$ relationship into two groups (FIG. 2(a)). When $\alpha_{\text{eff}} < \alpha_c$, \mathcal{R} approximately scales with α_{eff} proportionally. When $\alpha_{\text{eff}} > \alpha_c$, \mathcal{R} approximately scales with $(\alpha_{\text{eff}})^{0.5}$ with a rather sharp division between the two. Here, the transitional aspect ratio α_c and the corresponding transitional normalized run-out distance \mathcal{R}_c can be seen as the critical aspect ratio and the critical run-out distance, respectively (FIG. 2(b)). Both α_c and \mathcal{R}_c vary as we change the size of the granular column. For instance, in FIG. 2(b), the transition happens at $\alpha_c \approx 8, \mathcal{R}_c \approx 5$ when $R_i/d = 2.5$, and happens at $\alpha_c \approx 2, \mathcal{R}_c \approx 3.5$ when $R_i/d = 17.5$.

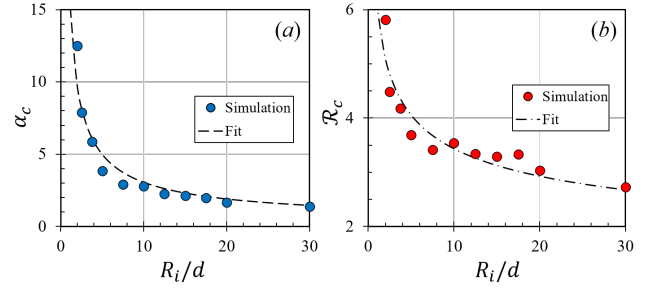


FIG. 3. (a) shows the relationship between transitional aspect ratio, α_c , and the relative column size, R_i/d . (b) plots the transitional normalized run-out distance, \mathcal{R}_c against R_i/d

We show, in FIG. 2(b), that a critical transition point (α_c and the corresponding \mathcal{R}_c) exists and also varies with different relative size R_i/d . Thus, $\mathcal{R} - \alpha_{\text{eff}}$ curve is dictated by the position of α_c and \mathcal{R}_c in a way that

$$\mathcal{R} = f(\alpha_{\text{eff}} - \alpha_c, \mathcal{R}_c, R_i/d). \quad (1)$$

Both α_c and \mathcal{R}_c decrease with an increase of R_i/d . In FIG. 3, based on the relationship between α_{eff} and \mathcal{R} in FIG. 2(a), we plot the relationship between α_c and R_i/d and the relationship between \mathcal{R}_c and R_i/d , respectively. Thus, we could write α_c and \mathcal{R}_c as functions of the relative column size, where, when R_i/d approaches infinity, both α_c and \mathcal{R}_c converge to $\alpha_{c\infty}$ and $\mathcal{R}_{c\infty}$, as shown by

$$\alpha_c = \alpha_{c\infty} + a_1 \left(\frac{R_i}{d} \right)^{b_1}, \quad (2a)$$

$$\mathcal{R}_c = \mathcal{R}_{c\infty} + a_2 \left(\frac{R_i}{d} \right)^{b_2}, \quad (2b)$$

where $\alpha_{c\infty} = 0.2$ and $\mathcal{R}_{c\infty} = 0.732$ are the fitted critical aspect ratio and the corresponding critical run-out distance, respectively, when the relative column size R_i/d goes to infinity, and both parameters are fitted values. Also, $a_1 = 16$, $b_1 = -0.75$, $a_2 = 5.4$, and $b_2 = -0.3$ are fitting parameters. The fitted curves of α_c and \mathcal{R}_c are

the dashed curve in FIG. 3(a) and the dash-dot curve in FIG. 3(b).

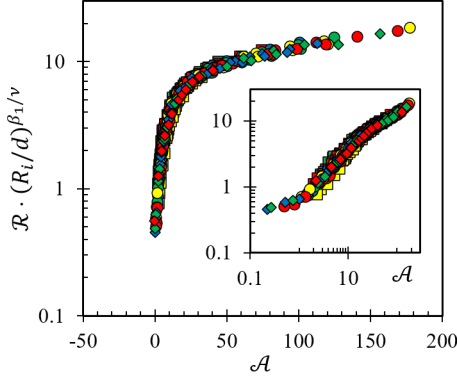


FIG. 4. The figure shows the relationship between $\mathcal{R}(R_i/d)^{\beta_1/\nu}$ and $\mathcal{A} = (\alpha_{\text{eff}} - \alpha_{c\infty})(R_i/d)^{1/\nu}$, with $\nu = 1.39$ and $\beta_1 = 0.28$. The inset of the figure plots the same relationship in a log-log coordinate system.

The power-law decay of both α_c and \mathcal{R}_c with respect to R_i/d inspires us to perform finite-size analysis of the run-out distance of the collapse of granular columns based on our working hypothesis of a potential phase transition. As shown in FIG. 4, the normalized run-out distance, \mathcal{R} indeed exhibits excellent finite-size scaling, suggesting that the transitional aspect ratio, α_c , is critical. All the normalized run-out distance data collapse nicely onto a master curve in the form[26]

$$\mathcal{R} = \left(\frac{R_i}{d}\right)^{-\beta_1/\nu} \mathcal{F}_r \left[(\alpha_{\text{eff}} - \alpha_{c\infty}) \left(\frac{R_i}{d}\right)^{1/\nu} \right], \quad (3)$$

with the limiting scaling of the normalized run-out distance being $\mathcal{R} \sim \alpha_{\text{eff}} - \alpha_{c\infty}$, where $\nu = 1.39 \pm 0.14$ and $\beta_1 = 0.28 \pm 0.04$ are obtained to best collapse all the data. In FIG. 4, to better represent the results, we took $\mathcal{A} = (\alpha_{\text{eff}} - \alpha_{c\infty})(R_i/d)^{1/\nu}$ as the x -axis. Since the system is axisymmetric, the scaling solution for the collapse of granular materials shows similar phenomena in the scaling solutions for connectivity of two-dimensional continuous random networks[26], where the scaling parameters $\nu = 1.33$ and $\beta = 0.1389$. This indicates that the flowing behavior of granular column collapse has strong correlations with the connectivity of grain contact networks. This also coincides with the suggestion made by Mehta[3] that the transport of grains takes place percolatively, especially in the context of avalanches.

We then investigate the strong force network of columns with different relative sizes at the very beginning of collapses (FIG. 5). In FIG. 5, we only plot the contact forces f that are larger than the mean contact force $\langle f \rangle$ linking the centroids of contacting particle pairs. The blue dashed lines represent the height that the strong force network can reach in the vertical direction,

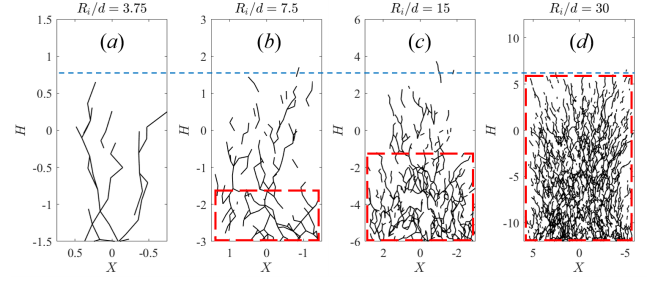


FIG. 5. Strong force network of granular columns with the same initial aspect ratio but different relative sizes at the beginning of collapse. Solid lines in the figure represent the link between contacting particles with magnitude of contact forces larger than the mean magnitude of contact forces. Blue dashed line represents the height where strong force network can propagate in the vertical direction, and red dashed lines denote the region where the strong force network could occupy the whole width. The height of the red dashed region is h_s , which represent the height of fully occupied strong force networks.

while the red dashed rectangles denote the region which the strong force network could occupy the whole cross-section. As we increase the relative size of the column, the height of the strong force network remains almost unchanged. However, the horizontal occupation of the strong force network is strengthened with the increase of the relative column size. This indicates that larger columns could form better-connected strong force networks in the horizontal direction at the beginning of the column collapse, and therefore might have the capacity to drive the system to flow further than smaller columns.

Equation 3 and the strong force network imply that a length scale exists during the collapse of granular columns in a form that the relative size of the length scale with respect to the column height has a power-law relationship with $\alpha_{\text{eff}} - \alpha_{c\infty}$,

$$\xi/H_i \sim (\alpha_{\text{eff}} - \alpha_{c\infty})^{-\zeta}, \quad (4)$$

where ζ is a fitting parameter for the length scale ξ , and ξ/H_i denotes the degree of occupation of sheared granular media along the height of initial granular column. To further investigate the length scale ξ associated with the collapse of granular columns, we choose four sets of simulations with different relative system sizes. We consider grain pairs along the vertical direction at the very beginning of the collapse when time $t = 0.05$ s, and define the corresponding correlation $G(z)$, which describes the correlation between particle pairs with vertical distance z , based on the equation proposed by Barker and Mehta[3, 27], by

$$G(z) = \frac{\langle \Delta z_i \Delta z_j \delta(|z_{ij}| - z) \Theta(|d_{ij} - 1/2|) \rangle}{\langle |\Delta z_i|^2 \rangle}, \quad (5)$$

where Δz_i and Δz_j are the vertical displacements of particle i and j after one time step (e.g. $\Delta z_i = v_i \Delta t$

where v_i is the velocity of particle i and Δt is the time step), z_{ij} is the vertical distance between two particles, z is the vertical displacement between particles, and $d_{ij} = \sqrt{(x_i - x_j)^2 + (y_i - y_j)^2}$ is the horizontal distance between two particles. Here, $\delta(\cdot)$ is a rectangular function, where the function is equal to one when $z - 0.5d < |z_{ij}| \leq z + 0.5d$ and equal to zero elsewhere, and $\Theta(\cdot)$ is the Heaviside step function. This definition ensures that the averages run over all displacements of sphere pairs in the vertical direction. The correlation function $G(z)$ shows how particles influence each other in z -direction.

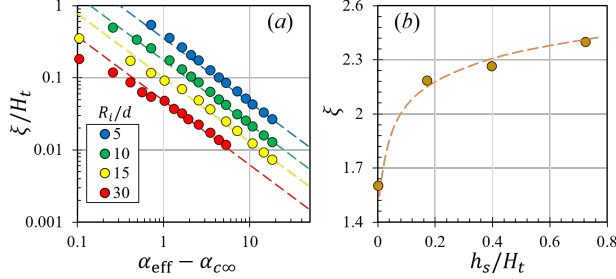


FIG. 6. (a) The relationship between ξ/H_t and $\alpha_{\text{eff}} - \alpha_{c\infty}$ when ξ and H_t are measured at the beginning of the granular collapse, where ξ is the correlation length scale, and H_t is the height of the system at the time we take the measurement. We only measured ξ for four different system sizes and plot the results using circle markers. Meanwhile, the fitted power-law relationships are denoted using dashed lines. (b) shows the relationship between ξ and h_s/H_t , where h_s is the height of the fully occupied strong force region in FIG. 5.

The displacement correlation function can be fitted with an exponential equation $G(z) = A \cdot \exp(-z/\xi)$, where ξ can be seen as a correlation length scale associated with the displacement correlation among particles during the collapse of granular columns, and A is a fitting parameter. The occupation of correlated grains across the height of a granular column, represented by ξ/H_t where H_t here is the height of the column at the time when we measure the correlation length scale (since ξ is measured at the very beginning of the collapse, $H_t \approx H_i$), implies the collective motion of particles during a collapse of granular columns. Thus, we plot the relationship between ξ/H_t and $\alpha_{\text{eff}} - \alpha_{c\infty}$ in Fig. 6(a), and determine that the ratio between correlation length scale and the system height shows power-law decay as we increase $\alpha_{\text{eff}} - \alpha_{c\infty}$, which is consistent with the finite-size scaling of both run-out behavior of granular column collapses, and $\zeta = 0.89$ in Eq. 4 best fits the power-law decay. When α_{eff} approaches $\alpha_{c\infty}$, ξ/H_t starts to deviate from the power-law relationship. This is due to the fact that, when the initial aspect ratio is too small, only several layers of particles present along the height of a granular column.

Additionally, we calculate the correlation length scales,

ξ , of the four cases shown in FIG. 5, and plot them against the ratio between the height of the fully occupied strong force region h_s and the column height H_t . We find that, as we increase the relative column size, not only does the height of fully occupied strong force region increase, but the correlation length scale also increases accordingly. This implies that larger system could help establish a better correlated moving mass, and as we increase the initial aspect ratio, columns with larger relative size, where well-correlated moving mass is easier to be established, would experience the phase transition from quasi-static collapse to inertial collapse earlier than smaller systems. To further analyze the phase transition associated with granular column collapses, we have to conduct rigorous investigations on the mean-field theory in future studies.

Summary.— Previous research concluded that we could combine the influence of initial and boundary conditions and the initial column aspect ratio to determine the normalized run-out distance with an effective aspect ratio, α_{eff} , which introduced a universal relationship to link the behavior of granular column collapses in three different collapsing regimes (quasi-static, inertial, and liquid-like)[22]. In this paper, we further investigated the size effect associated with the collapse of granular columns based on the previous research. Our research is performed with DEM simulations of Voronoi-based spheropolyhedron particles. We found that the transition point in $\mathcal{R} - \alpha_{\text{eff}}$ space, which distinguishes the inertial collapse regime from the quasi-static collapse regime, varies as we change the relative system size R_i/d . Both \mathcal{R}_c and α_c experience power-law decay with respect to R_i/d , which implies possible finite-size scaling for the normalized run-out distance \mathcal{R} .

Similar to the finite-size analysis of the jamming transition of granular materials[28], where the stress scales with the solid fraction $\phi - \phi_{c\infty}$, we took the previously determined effective aspect ratio α_{eff} as the key parameter, and discovered that both the run-out distance of granular column collapse and the energy consumption of it follows strong finite-size scaling. Interestingly, the scaling parameters we discovered for the finite-size scaling of the run-out distance of granular column collapses are similar to those presented in percolation problems of two-dimensional random networks[26], which may imply that the behavior of granular column collapses is strongly influenced by the contact network presented inside the column during the collapse. Additionally, to better understand the scaling of granular column collapses, we further analyze the correlation length scale at the very beginning of the collapse. Simulation results show that, as we increase $\alpha_{\text{eff}} - \alpha_{c\infty}$, the length scale ξ/H_t shows a power-law decay with scaling parameter $\zeta \approx 0.89$. This study is based on our previous work where we introduced a physics-based dimensionless number (ratio between inertial effects and frictional effects) to describe the behav-

ior of granular column collapses, and we further expand our analysis to include the size effect, which is crucial to applications in engineering, such as chemical engineering, food processing, civil engineering. We also associate the size effect to the strong force networks at the beginning of the column collapse to show that larger column size results in a well percolated strong force network which may contribute to relatively larger run-out distances. However, the granular system we are studying is still axisymmetric, and our preliminary results show intriguing phenomena when the cross-section of a granular column is no longer axisymmetric. Further investigations will be presented in future publications.

The authors acknowledge the financial support from Westlake University and thank the Westlake University Supercomputer Center for computational resources and related assistance. The author also thank Raphael Blumenfeld, Alexey Kavokin, Lydie Staron, Laurent Lacaze, John Hinch, and Howard Stone for helpful discussions on this paper. H.E. Huppert acknowledges with gratitude the hospitality of his co-authors while he was at Westlake University.

* Also at Key Laboratory of Coastal Environment and Resources of Zhejiang Province (KLaCER), School of Engineering, Westlake University

† s.torres@westlake.edu.cn

- [1] E. Guyon, J.-Y. Delenne, and F. Radjai, *Built on Sand: The Science of Granular Materials* (MIT Press, 2020).
- [2] G. D. R. MiDi, Euro Phys J E **14**, 341 (2004).
- [3] A. Mehta, *Granular Physics* (Cambridge University Press, 2007).
- [4] T.-T. Vo, P. Mutabaruka, S. Nezamabadi, J.-Y. Delenne, and F. Radjai, Phys. Rev. E **101**, 032906 (2020).
- [5] L. Zhang, Y. Wang, and J. Zhang, Phys. Rev. E **89**, 012203 (2014).
- [6] P. Jop, Y. Forterre, and O. Pouliquen, Nature **441**, 727 (2006).
- [7] M. Trulsson, B. Andreotti, and P. Claudin, Physical Review Letters **109**, 118305 (2012).
- [8] T. Man, *Rheology of Granular-Fluid Systems and Its Application in the Compaction of Asphalt Mixtures*, Ph.D. thesis, University of Minnesota (2019).
- [9] T.-T. Vo, Journal of Rheology **64**, 1133 (2020).
- [10] T.-T. Vo, S. Nezamabadi, P. Mutabaruka, J.-Y. Delenne, and F. Radjai, Nature Communications **11** (2020), 10.1038/s41467-020-15263-3.
- [11] R. Zenit, Physics of Fluids **17**, 031703 (2005).
- [12] E. L. Thompson and H. E. Huppert, Journal of Fluid Mechanics **575**, 177 (2007).
- [13] L. Lacaze and R. R. Kerswell, Physical Review Letters **102**, 108305 (2009).
- [14] L. Rondon, O. Pouliquen, and P. Aussillous, Physics of Fluids **23**, 073301 (2011).
- [15] P.-Y. Lagr e, L. Staron, and S. Popinet, Journal of Fluid Mechanics **686**, 378 (2011).
- [16] G. Lube, H. E. Huppert, R. S. J. Sparks, and M. A. Hallworth, Journal of Fluid Mechanics **508**, 175 (2004).
- [17] G. Lube, H. E. Huppert, R. S. J. Sparks, and A. Freundt, Physical Review E **72**, 041301 (2005).
- [18] E. Lajeunesse, J. Monnier, and G. Homsy, Physics of Fluids **17**, 103302 (2005).
- [19] J. Warnett, P. Denissenko, P. Thomas, E. Kiraci, and M. Williams, Granular Matter **16**, 115 (2014).
- [20] J. M. Warnett, *Stationary and rotational axisymmetric granular column collapse*, Ph.D. thesis, University of Warwick (2014).
- [21] M. Cabrera and N. Estrada, Phys. Rev. E **99** (2019), 10.1103/PhysRevE.99.012905.
- [22] T. Man, H. E. Huppert, L. Li, and S. A. Galindo-Torres, Granul. Matt. (accepted) (2021), 10.1007/s10035-021-01112-7.
- [23] S. A. Galindo-Torres, X. Zhang, and K. Krabbenhoft, Phys. Rev. Appl. **10**, 064017 (2018).
- [24] S. A. Galindo-Torres and D. Pedroso, Physical Review E **81**, 061303 (2010).
- [25] S. Galindo-Torres, Computer Methods in Applied Mechanics and Engineering **265**, 107 (2013).
- [26] S. A. Galindo-Torres, T. Molebatsi, X.-Z. Kong, A. Scheuermann, D. Bringemeier, and L. Li, Phys Rev E **92**, 041001 (2015).
- [27] G. C. Barker and A. Mehta, Phys. Rev. A **45**, 3435 (1992).
- [28] H. Liu, X. Xie, and N. Xu, Phys. Rev. Lett. **112**, 145502 (2014).